Thermoelectric properties–texture relationship in highly oriented $Ca_3Co_4O_9$ composites

E. Guilmeau and R. Funahashi[a)]
National Institute of Advanced Industrial Science and Technology, Midorigaoka, Ikeda, Osaka 563-8577, Japan

M. Mikami
CREST, Japan Science and Technology Agency, Ikeda, Osaka 563-8577, Japan

K. Chong
Osaka Electro-Communication University, Neyagawa, Osaka 572-0833, Japan

D. Chateigner
CRISMAT-ENSICAEN Laboratory, UMR CNRS 6508, 6 Bd. Marechal Juin, 14050 Caen Cedex, France

(Received 4 March 2004; accepted 21 June 2004)

The correlation between thermoelectric properties and texture strength is discussed within the framework of $Ca_3Co_4O_9$ textured ceramics. Based on an innovative method of x-ray diffraction analysis, the distribution density (i.e., the degree of orientation) of composite material composed of $Ca_3Co_4O_9$ powder and single crystals was determined. Electrical resistivity of the prepared composites was shown to be reduced with increasing single crystals weight ratios and, in parallel, was directly correlated to an improvement of grain alignment. The incorporated single crystals help the texture development of the powder via an enhanced stacking of grains and fulfill a role as bypasses of the grain boundaries. This letter highlights the value of quantitative texture analysis to explain the evolution of anisotropic physical properties, as demonstrated here concerning textured thermoelectric materials. © *2004 American Institute of Physics*. [DOI: 10.1063/1.1785286]

Thermoelectric (TE) power generation has the potential to provide an energy source in the next few decades. The recent discoveries of large thermopower coexisting with low electrical resistivity in cobaltite layered structures, such as Na_xCoO_2 (Ref. 1) and $Ca_3Co_4O_9$ (Co349),[2–4] opened the way to the exploration of oxide thermoelectric materials and the development of polycrystalline bulk materials for potential applications. Due to its relatively good TE performance and resistance to humidity, the Co349 compound has attracted the interest of many researchers exploring various ways of improving the TE properties of ceramics for TE devices. One of the well-known ways for the enhancement of transport properties consists of the alignment of platelike grains in the bulk materials due to the highly anisotropic properties of the Co349 layered structure.[3] Several research groups have reported the preparation of Co349 textured ceramics.[5–8] Notably, it has been reported[8] that Co349 hot-pressed ceramics composed of powder and single crystals (SCs) show lower resistivity than those without SCs. The reason has been speculated to be improved grain alignment, but has yet to verified. The Lotgering factor,[9] usually used in literature is, however, not suitable for this purpose. For instance, when only $\{00\ell\}$ peaks are observed, the Lotgering factor takes the value of 1. But many different textures can be stabilized exhibiting only $\{00\ell\}$ peaks in a given 2θ range, with various dispersions. The correlation between the Lotgering factor and a quantitative description of the texture is then, if it exists at all, subject to caution. Thus, a more effective texture analysis technique is necessary to find the optimum preparation conditions. We propose here an approach to quantitatively determine the texture strength, i.e., the degree of orientation of the bulk materials. Analogous to previous works on $(Bi,Pb)_2Sr_2Ca_2Cu_3O_{10+\delta}$ superconducting ceramics,[10] the method would appear effective in determining the fiber texture of TE compounds in order to investigate the influence of grain alignment on TE properties. We detail the methodology and its impact on the interpretation of transport properties in Co349 powder/SC composites.

A precursor powder with the composition $Ca_{2.7}Bi_{0.3}Co_4O_9$ was calcined at 800 °C for 10 h in air, then pelletized, and fired at 800 °C for 20 h under an O_2 gas flow. The sintered samples were then ground manually and the resulting platelike grain powder was uniaxially pressed into pellets ($\varnothing = 20$ mm, $h = 0.2$ mm). These pellets were then placed in a 25 mm square molder with $Ca_3Co_4O_9$ SCs (Ref. 11) introduced between each pellet. The maximum in-plane size of the SCs is around 2 mm, the thickness is about 0.05 mm and the weight ratio varies from 0% to 20%. The resulting square pellets were then subjected to hot-forging treatment at 850 °C for 20 h under 300 kg of uniaxial pressure.

Texture analysis was performed by x-ray diffraction (XRD) using a curved position-sensitive detector (INEL CPS 120) spanning 120° in 2θ. This configuration allows rapid measurement (i.e., without Bragg angle scanning) of the whole diffraction pattern at each sample orientation, i.e., tilt angle (χ) between the flat sample surface and the diffraction plane and azimuthal angle (φ) around the sample normal. A 1×1 mm collimated beam was used and the sample holder was vibrated slightly (±1 mm) in order to ensure that the entire beam intersected the flat sample (even at high sample tilt angles) and that the number of irradiated crystallites was statistically relevant. Since the samples have an axially symmetric (fiber) texture (i.e., random in-plane distribution of

a)Electronic mail: funahashi-r@aist.go.jp

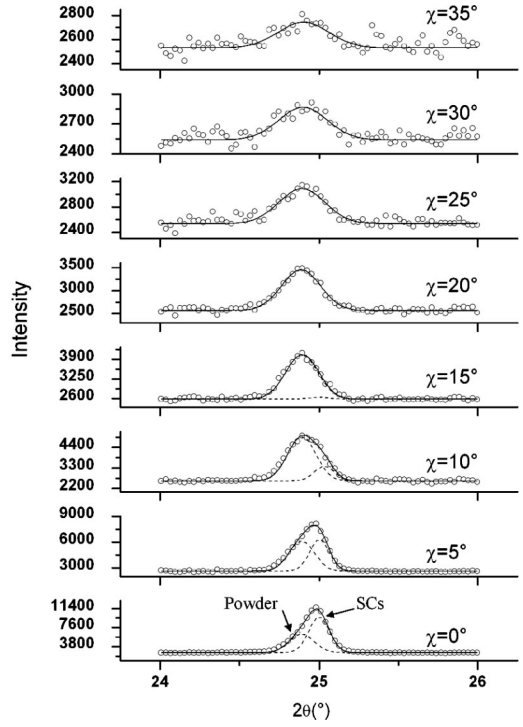

FIG. 1. Experimental (circles) and Gaussian fits (solid and dashed lines) of the {003} diffraction peak for various χ angles (20 wt % of SCs). Double peak shape until $\chi=15°$, single peak shape for $\chi=20°$ to 35°.

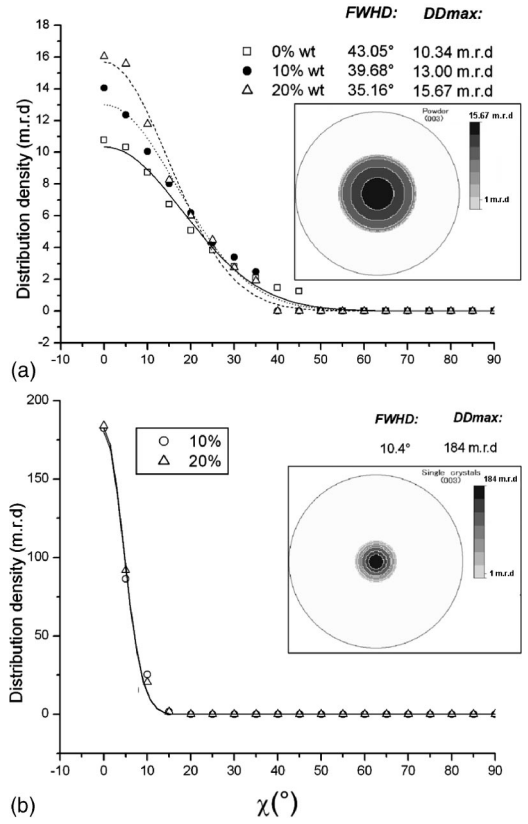

FIG. 2. Distribution density vs χ-angle curves of (a) the powder component for various contents of SCs and (b) the SCs component (10 or 20% wt of SC). FWHD and DD_{max} values are included. Insets represent the reconstructed {003} pole figures related to (a) the powder and (b) the SC component. Logarithmic density scale, equal area projection.

crystallite *a* and *b* axes), the complete texture determination can be obtained only by measuring the inclination of $\{00\ell\}$ crystallographic planes off the sample surface, the φ rotation being unnecessary. This was achieved by selecting the {003} reflection using an incidence angle ω of 12.5° and scanning the tilt angle from $\chi=0$ to $\chi=60°$, in 5° steps, with an integration time of 1 h for each tilt angle orientation. The {003} Gaussian integrated peaks were used as inputs to reconstruct χ-scans which represent the $\{00\ell\}$ plane dispersions of the crystallites. These χ-scans were normalized into distribution density $[D_{hk\ell}(\chi,\varphi)]$ scans using the direct normalization procedure

$$D_{hk\ell}(\chi,\varphi)=\frac{I_{hk\ell}(\chi,\varphi)}{I^{r}_{hk\ell}}, \tag{1}$$

in which $I_{hk\ell}(\chi,\varphi)$ is the integrated intensity of the $\{hk\ell\}$ peak (in our case {003}) for the (χ,φ) orientation of the sample and $I^{r}_{hk\ell}$ would be the integrated intensity of the same sample without texture. Using such an approach, a sample without any texture has densities of 1 multiple of a random distribution (m.r.d.) regardless of the (χ,φ) orientation, and a textured sample exhibits minima and maxima of the density values over χ angles. The calculation of $I^{r}_{hk\ell}$ (Ref. 12) is operated using

$$I^{r}_{hk\lambda}=\frac{\sum_{\chi\varphi} I_{hk\ell}(\chi,\varphi)\sin\chi\Delta\chi\Delta\varphi}{\sum_{\chi\varphi}\sin\chi\Delta\chi\Delta\varphi}, \tag{2}$$

where $\sin\chi\Delta\chi\Delta\varphi$ represents the unit solid angle of the pole sphere in which each integrated intensity is distributed. For measurement of constant angular steps ($\Delta\chi$ and $\Delta\varphi$), Eq. (2) is simplified to:

$$I^{r}_{hk\lambda}=\frac{\sum_{\chi} I_{hk\ell}(\chi)\sin\chi}{\sum_{\chi}\sin\chi}. \tag{3}$$

The distribution density versus χ-angle curve is then fitted as Gaussian orientation distributions. The maximum of the distribution density (DD_{max}) and the full width at half maximum of the distribution (FWHD) represents the (00l) orientation distribution and were used as parameters for a quantitative appreciation of the crystallite dispersion. The electrical resistivity along the *ab* plane direction (ρ_{ab}) was measured using a conventional four-probe dc technique from room temperature to 1000 K in air. This resistivity corresponds to the averaged *ab*-plane resistivity of the structure over the plane orientations. The Seebeck coefficient was calculated from a plot of TE voltage against temperature differential as measured in the 373–1073 K range in air using an instrument designed by our laboratory.[13]

Shown by Fig. 1 is the {003} diffraction peak variation with χ fitted as a two-Gaussian-component peak shape (sample with 20 wt % of SC). Two interesting features can be noticed. First, the high $\{00\ell\}$ degree of orientation in the composite material is highlighted by the strong decrease of the diffracted intensity with increasing χ angles. Second, an asymmetric peak shape is observed for lower χ positions, as a sign of the two components present in the material, i.e., the powder and the SCs. The difference in composition between the powder and the SCs ($Ca_{2.7}Bi_{0.3}Co_4O_9$ and $Ca_3Co_4O_9$, respectively) is the origin of this asymmetry. As was been re-

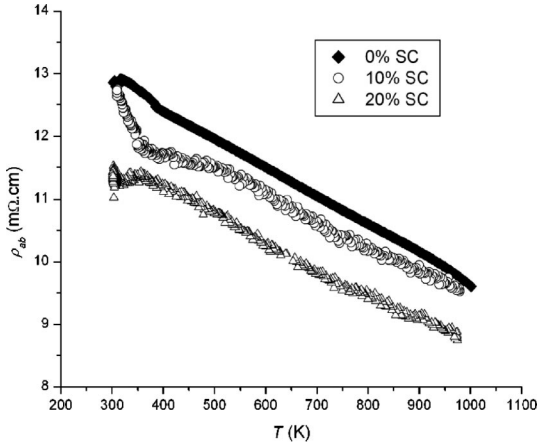

FIG. 3. Electrical resistivity vs temperature curves for varying SC contents in the composites.

ported by Mikami *et al.*,[14] the substitution of Bi in the rock-salt layer induces an increase of the c unit-cell parameter. As a consequence, the undoped SCs exhibit $\{00\ell\}$ lines shifted to larger 2θ values compared to the doped powder. We deconvoluted these two contributions by a double-Gaussian peak shape for the 10% and 20% composite samples whereas a single-Gaussian peak shape was used for the 0% sample. From a qualitative point of view, the rapid decrease of the $\{003\}$-SC peak highlights its strong texture compared to the powder which exhibits $\{003\}$ diffracted intensities up to 35%.

From the deconvoluted peaks, the normalization procedure described above allows reconstruction of the χ-scans which represent the $\{00\ell\}$ plane dispersions of both the powder and SC crystallites. Figure 2(a) represents distribution density curves of the powder component in three samples containing different SC weight percentages. The DD_{max} and FWHD parameters, representing the degree of orientation, are included in the graph. Without ambiguity, the SC incorporation in the bulk materials has a significant influence on the improvement of the texture strength. The large surface of the SCs probably acts as a support and pressure template to develop the texture of the powder around them. By increasing the amount of SCs in the material, the total contact surface is increased and results in an improvement of the degree of orientation. The development of stronger powder texture strength is also facilitated by the SCs' high degree of orientation. As shown in Fig. 2(b), the distribution density curves of the SCs, measured in both 10% and 20% samples, presents a maximum around 180 m.r.d., value almost 12 times larger than the powder. The representation of the pole figures, calculated from the χ-scans, illustrates clearly the texture of both components of the material [Insets of Figs. 2(a) and 2(b)]. Whereas the (003) pole of SCs is narrow, the larger crystallite angular dispersion of the powder induces a broader pole with a density of zero for $\chi > 35°$.

Finally, we demonstrate the relationship of transport properties to texture in these composites. As shown in Fig. 3, the evolution of the electrical resistivity follows the degree of orientation well. The improved alignment of powder grains in proximity to the SCs in the composite facilitates the current transport between the grains. Also, as speculated previously,[8] the SCs probably act as bypasses for the current and reduce the detrimental effect of grain boundaries. On the other hand, the apparent density of the samples decreases with increasing SC ratios ($d_{0\%}=4.64$ g/cm^3, $d_{10\%}=4.37$ g/cm^3, and $d_{20\%}=4.28$ g/cm^3). The difference in density between the powder (Bi doped) and the SC (undoped) could be a possible hypothesis to explain this evolution. However, the respective corresponding theoretical densities are 5.05, 5.01, and 4.97 g/cm^3 demonstrating that this difference indeed comes from a porosity increase. This is consistent with scanning electron microscopy observation showing that the stacking between the large SCs is defective and represents the major contribution for the density decrease. This trend, which normally causes a drastic increase of electrical resistivity,[15,16] is, in this case, thwarted by the improvement of grain alignment. In addition, as the Seebeck coefficient is nearly unchanged between the three samples (~ 180 μV/K at 973 K), the resulting power factor (PF_{ab}) is increased and reaches 0.35 mW/mK^2 for the sample containing 20 wt % of the SCs.

In conclusion, the relationship between SC incorporation, texture, and TE properties has been clearly shown and proves the effectiveness of the quantitative texture analysis for a better understanding of physical properties and design of improved TE bulk materials. The results highlighted the effect of improved grain alignment on bulk resistivity measurements. Our method of analysis, particularly suitable in the case of this study on $Ca_3Co_4O_9$ polycrystalline materials, is also a rapid and effective way of characterizing preferred orientations of materials for which texture development is necessary to attain macroscopic properties comparable to the intrinsic crystallographic ones. Finally, the information obtained through this study should allow consideration of synthesis of improved materials with stronger texture strengths and TE performances.

D.C. greatly acknowledges the French Ministère de l'Education Nationale et de la Recherche and the Délégation Régionale à la Recherche et à la Technologie for their financial support.

[1] I. Terasaki, Y. Sasago, and K. Uchinokura, Phys. Rev. B **56**, R12685 (1997).
[2] S. Li, R. Funahashi, I. Matsubara, K. Ueno, and H. Yamada, J. Mater. Chem. **9**, 1659 (1999).
[3] A. C. Masset, C. Michel, A. Maignan, M. Hervieu, O. Toulemende, F. Studer, B. Raveau, and J. Hejtmanek, Phys. Rev. B **62**, 166 (2000).
[4] R. Funahashi, I. Matsubara, H. Ikuta, T. Takeuchi, U. Mizutani, and S. Sodeaka, Jpn. J. Appl. Phys., Part 2 **39**, L1127 (2000).
[5] T. Tani, H. Itahara, C. Xia, and J. Sugiyama, J. Mater. Chem. **13**, 1865 (2003).
[6] Y. Zhou, I. Matsubara, S. Horii, T. Takeuchi, R. Funahashi, M. Shikano, J. Shimoyama, K. Kishio, W. Shin, N. Izu, and N. Murayama, J. Appl. Phys. **93**, 2653 (2003).
[7] J.-W. Moon, D. Nagahama, Y. Masuda, W.-S. Seo, and K. Koumoto, J. Ceram. Soc. Jpn. **109**, 647 (2001).
[8] R. Funahashi, S. Urata, T. Sano, and M. Kitawaki, J. Mater. Res. **18**, 1646 (2003).
[9] F. K. Lotgering, J. Inorg. Nucl. Chem. **9**, 113 (1959).
[10] Guilmeau, D. Chateigner, and J. G. Noudem, Semicond. Sci. Technol. **15**, 1436 (2002).
[11] M. Shikano and R. Funahashi, Appl. Phys. Lett. **82**, 1851 (2003).
[12] J. R. Holland, Adv. X-Ray Anal. **7**, 86 (1964).
[13] M. Mikami, R. Funahashi, M. Yoshimura, Y. Mori, and T. Sasaki, J. Appl. Phys. **94**, 6579 (2003).
[14] M. Mikami, K. Chong, and R. Funahashi (unpublished).
[15] Y. Masuda, D. Nagahama, H. Itahara, T. Tani, W.-S. Seo, and K. Koumoto, J. Mater. Chem. **13**, 1094 (2003).
[16] H. Itahara, K. Fujita, J. Sugiyama, K. Nakamura, and T. Tani, J. Ceram. Soc. Jpn. **111**, 227 (2003).